J Wood Sci (2009) 55:264–272
DOI 10.1007/s10086-009-1031-7

ORIGINAL ARTICLE

Jung-Kwon Oh · Kugbo Shim · Kwang-Mo Kim · Jun-Jae Lee

Quantification of knots in dimension lumber using a single-pass X-ray radiation

Received: July 29, 2008 / Accepted: March 12, 2009 / Published online: May 29, 2009

Abstract The knot depth ratio (KDR) evaluation method was designed to quantitatively evaluate the amount of knot in dimension lumber by a single-pass X-ray radiation. To verify the proposed method, KDR values for 38-mm-thick specimens were predicted, and they were compared with the actual measured KDR values. The knot is surrounded by the transition zone, and the density of the knot and the transition zone is higher than the clear wood. Because the average density of the transition zone was similar to the knot density, it was found that the proposed method gives the KDR values for the knot area including the transition zone. The coefficients of determination between the predicted and measured KDR values were 0.87 and 0.83 for Japanese larch and red pine specimens, respectively. Using the KDR information, the ratio of knot area including transition zone to cross-sectional area was calculated. The presence of latewood and earlywood in the same path of the X-ray radiation caused discrepancies in the estimation of KDR values because the density of latewood is much higher than that of earlywood. Fortunately, latewood and earlywood are repeated in a cross section, so the amount of overestimation and underestimation was expected to be nearly identical. As expected, the relationship between the predicted area ratio and the real area ratio of knot and transition zone was strong with R^2 values of 0.89 and 0.93 for Japanese larch and red pine specimens, respectively.

Key words Knot · Knot depth ratio · X-ray · Defect · Image analysis

K. Shim · K.-M. Kim
Department of Forest Products, Korea Forest Research Institute, Seoul 130-712, Republic of Korea

J.-K. Oh · J.-J. Lee (✉)
Research Institute for Agriculture and Life Sciences, Department of Forest Sciences, Seoul National University, San 56-1 Sillim 9 dong Gwanak-gu, Seoul 151-921, Republic of Korea
Tel. +82-28-80-4782; Fax +82-28-71-0156
e-mail: junjae@snu.ac.kr

Introduction

Knots are almost always present in lumber and are known to be the most serious defect, because they greatly reduce the strength of lumber and the quality of products. Therefore, nondestructive evaluation of knots is crucial for estimation of lumber strength and yield of wood.

Riberholt and Madsen[1] reported that the failure of lumber is primarily initiated at the weakest cross section that corresponds to the largest knot or a group of knots. In the destructive bending test, failure is almost exclusively caused by knots. Schniewind and Lyon[2] tested redwood timber and in 95% of the cases, failure occurred at knots or local slope of the grain, which was mostly related to the knots. In a study by Johansson et al.,[3] 91% of failures were caused by knots.

In order to evaluate knots, there are various nondestructive evaluation methods such as acousto-ultrasonic[4] and microwave scanning,[5] stress wave propagation,[6] and image processing using optical instruments.[7] However, these studies focused only on detection of knots.

In general, the knot is regarded as a loss of cross section. Because knots are less resistant to stress than clear wood, the strength of lumber is inversely proportional to the knot area ratio (KAR), which is defined as the ratio of knot area to the cross-sectional area.[2] For instance, there are three shapes of knot as shown in Fig. 1. Among the three lumbers, the lumber containing the largest knot area (bottom in Fig. 1) was expected to be the weakest. However, most current nondestructive methods can determine the presence of knots and cannot quantify the amount of knots in the lumber thickness. Consequently, these knots cannot be distinguished from each other and may be regarded as the same size. However, because the KARs are different from each other, these lumbers show different strengths.

Schniewind and Lyon[2] estimated the KAR using the knot information observed on the surface of the lumber. The value of the KAR was correlated with the strength of the lumber. The current visual grading rules are also based on the KAR concept, such as *Standard Grading Rules for*

Canadian Lumber 2003 and *Western Lumber Grading Rules 2005*.[8] Because the naked eye can only inspect the outer appearance of the lumber and not the inner part, it is very difficult to measure the KAR in a cross section through visual inspection. Hence, the grading rules provide an alternative method to measure the knot size to be observed on the surface of the lumber. However, Madsen[9] concluded that the current visual grading rules cannot classify lumber according to strength. If the knot area in a cross section can be quantified with high accuracy, the accuracy of the strength prediction was also expected to improve.

In a different approach, X-rays can be used to inspect the inner part of the lumber. When X-rays pass through the lumber, part of the radiation energy is absorbed by the lumber and only the remaining part reaches the detector. The amount of absorbed energy depends on the density of the section of wood through which the X-ray passed. This density can be calculated using the attenuation equation of Beer's Law and X-ray radiography.[10,11] It is well known that the density of knots is twice that of normal wood.[12] The locations and sizes of knots can be identified by the presence of areas with high wood density.[13]

Computed tomography (CT) using X-rays can also identify defects in structural timber.[14–16] It is clear that CT scanning can also distinguish between three knots in Fig. 1. CT technology gives comprehensive and detailed information inside wood, but it requires repeated X-ray radiation and considerable time. In addition, simpler information, such as KAR, is adequate and desirable in practical situations.

In order to predict the strength of lumber more precisely, it is very important to evaluate the quantity of knot in a cross section. Therefore, this study was intended to predict the geometric amount of knot in the thickness of lumber using a single-pass X-ray radiation.

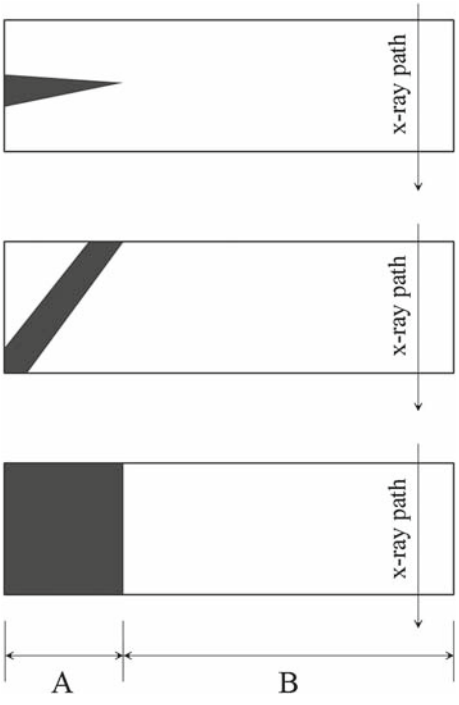

Fig. 1. Cross-sectional view of an example for the different knot shapes. *A*, The zone identified as a knot by knot detection; *B*, the zone identified as a clear part by knot detection

Materials and methods

Measurement of knot density

Knot density was measured by converting the X-ray image of a 10-mm-thick specimen into density. To verify density measurement using X-ray radiation, 19 wood specimens (10 mm thickness) were prepared. To provide a large variation in density, some samples contained knots and juvenile wood, and various wood species of Japanese larch (*Larix kaempferi*), Japanese cedar (*Cryptomeria japonica*), and red pine (*Pinus densiflora*) were used (Table 1). Because X-ray attenuation depends on the thickness of the specimen, the use of different thicknesses is required to verify the method. Twenty-four 38-mm-thick specimens were also prepared (Table 1).

X-ray scanning equipment consisted of an X-ray tube, a shield to protect the inspector, and an X-ray detector (Figs. 2 and 3). A Thales image intensifier (TH9429) was used as the X-ray detector. This detector can produce an X-ray digital image immediately, and no developing or printing is required. The resolution of the X-ray images was 2.7 dots per millimeter. The densities of specimens were calculated using Beer's Law (Eq. 1).[10,11] The intensity of X-ray radiation was quantified using a surveymeter (RSM-300, Iljin Radiation Engineering). The mass attenuation coefficient was experimentally determined for each thickness of the specimen. In order to compare the density predicted by X-ray scanning with the real density, the air-dry densities of the same specimens were measured according to Eq. 2.

$$\rho = \frac{1}{\mu t}\left(\log\left(\frac{I_0}{I}\right)\right) \quad (1)$$

Table 1. Specimens used to verify density measurement by X-ray radiation

Thickness of specimen (mm)	Species	Total number of specimens	Number of specimens with knots	Number of specimens with pith
10	Japanese larch	7	2	1
	Japanese cedar	5	3	2
	Red pine	7	1	1
38	Japanese larch	7	1	1
	Japanese cedar	8	2	2
	Red pine	9	3	1

Fig. 2. Photograph of X-ray equipment

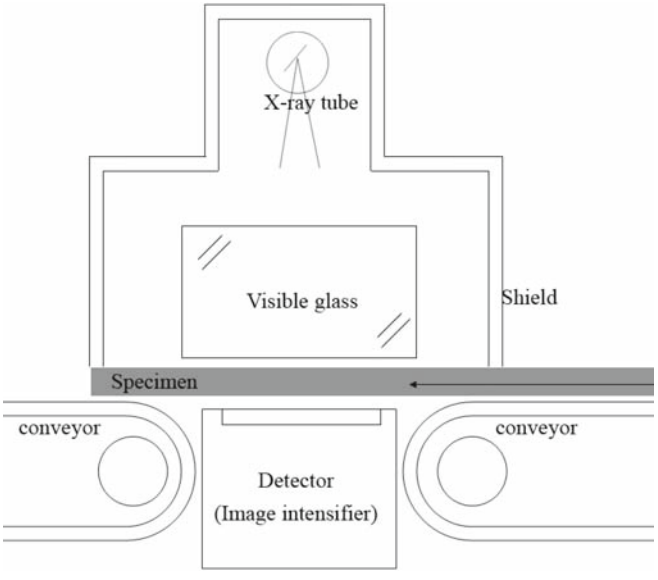

Fig. 3. Schematic drawing of X-ray test equipment

where ρ is the density evaluated by X-ray radiation (g/cm^3); μ is the mass attenuation coefficient (cm^2/g); t is thickness of the specimen (cm); I_0 is the intensity of incident radiation (Sv/h); I is the intensity of transmitted radiation (Sv/h).

$$D = \frac{W_{\text{air-dry}}}{V_{\text{air-dry}}} \tag{2}$$

where D is the air-dry density (g/cm^3); $W_{\text{air-dry}}$ is the weight of the specimen (g); $V_{\text{air-dry}}$ is the volume of the specimen (cm^3).

To measure the knot density, 54 knots of Japanese larch and 42 red pine knots of 10 mm in thickness were prepared. All specimens were prepared to have the knot penetrate the specimen thickness (10 mm) at a right angle (Fig. 4).

Specimens were set to allow X-rays to pass through the 10-mm thickness of the specimens. The X-ray images were converted into density by using Beer's Law (Eq. 1).[10,11] In

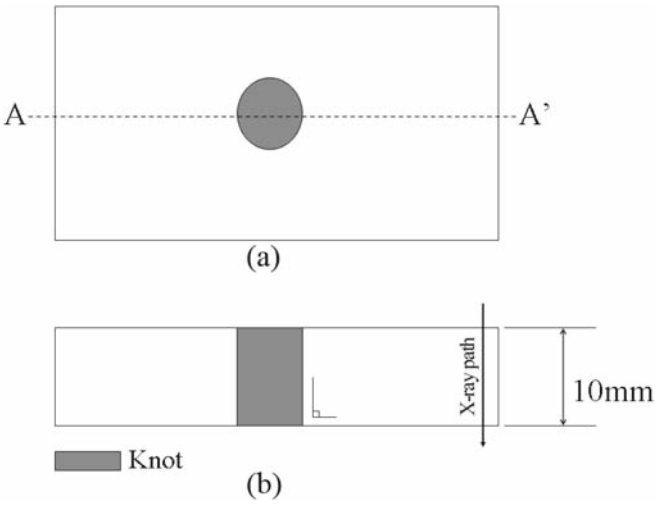

Fig. 4a, b. Specimen preparation for knot density measurement. **a** Wide face of the specimen. **b** Cross-sectional view at section A-A'

this study, the wide face of each specimen was divided into three zones: knot zone, transition zone, and clear part zone. The transition zone was defined as the area between the knot zone and the clear part zone. At first, the clearly identified knot zone and clear part were separated from other zones. All area not classified as clear part or knot zone was classified as transition zone. Some obscure areas were identified by observing the wide face of the specimen using a magnifying camera (ICSL-305, Sometech). The density of each zone was obtained by extracting the partial image for each zone from the raw X-ray image and converting the partial image into density by Beer's Law.

Verification of knot depth ratio prediction

Method to predict knot depth ratio

In Korea, Japanese larch and red pine are most frequently used for structural purposes. Therefore, 35 pieces of Japanese larch and 43 pieces of red pine were sampled from commercial mills. The size of each specimen was 38 × 140 × 3600 mm and the specimens were kiln-dried to an average moisture content of approximately 18%.

X-ray images were taken at cross sections containing knots. Specimens were set to allow X-rays to pass through the 38-mm thickness of the specimen. Eighty-five knots of Japanese larch and 73 knots of red pine were investigated. Using a knot detection algorithm,[13] two sheets of X-ray images were prepared for each specimen: knot X-ray image and clear part X-ray image.

The knot depth ratio (KDR) was defined as the ratio of knot thickness (t_{knot}) to lumber thickness (t) (Fig. 5, Eq. 3).

$$\text{KDR} = \frac{t_{\text{knot}}}{t} \tag{3}$$

Even though the densities of clear wood and knots vary over a wide range, it was assumed that the densities of both

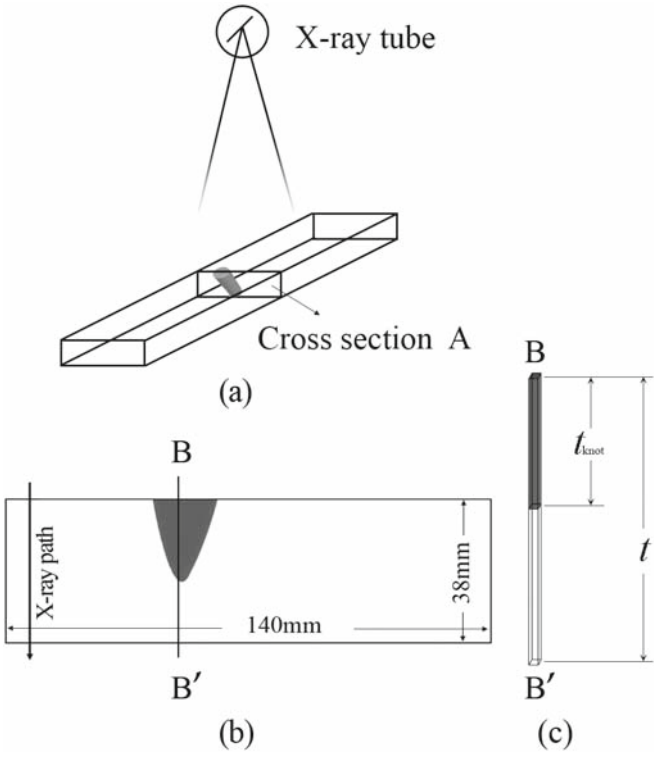

Fig. 5a–c. Schematic drawing of X-ray measurement test and unit volume for a cell of X-ray image. **a** Cross section containing a knot. **b** View of cross section A. **c** Unit volume for section B-B' (1 × 1 pixel × lumber thickness). t_{knot}, Thickness of knot; t, lumber thickness

clear parts and knots were uniform. The average density of the unit volume (Fig. 5c), which has one pixel by one pixel area of the X-ray image and the specimen thickness (t, 38 mm), can be calculated using Beer's Law (Eq. 1). If the densities of the clear part and the knot are uniform, the average density of the unit volume can be expressed as in Eq. 4, which can be rewritten as Eq. 5. The average clear part density (ρ_c) can be obtained from the clear part X-ray image extracted by the knot detection algorithm. Only the average knot density (ρ_k) is unknown. In this study, it was experimentally measured by using some specimens of the same species. Knot X-ray images were also converted into KDR values by using Eq. 5.

$$\rho = \rho_c(1 - \mathrm{KDR}_x) + \rho_k \mathrm{KDR}_x \tag{4}$$

$$\mathrm{KDR}_x = \frac{\rho - \rho_c}{\rho_k - \rho_c} \tag{5}$$

where KDR_x is the knot depth ratio evaluated by X-ray image analysis; ρ is the localized average density for a unit X-ray image cell of 1 pixel by 1 pixel; ρ_c is the average clear part density of the lumber; ρ_k is the average knot density.

Measurement of the real KDR

To verify the prediction of KDR, the cross section containing knots was cut after the X-ray measurement. The cut cross section was divided into three zones: knot zone, transition zone, and clear part zone (Fig. 6).

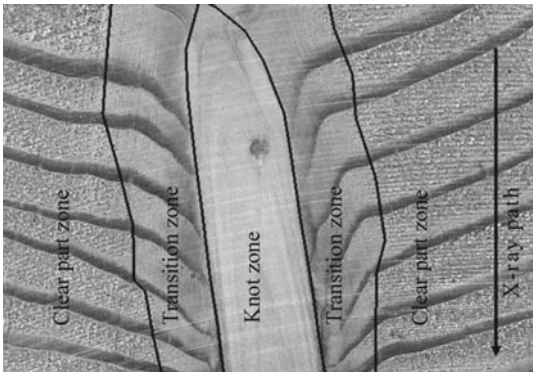

Fig. 6. Example of division of cross-sectional area into three zones (Japanese larch)

A mesh grid was overlaid on the cut cross section and the number of cells encompassed by knot was counted. The size of the mesh grid was 1.31 × 1.31 mm. Consequently, the KDR was obtained by dividing the number of knot cells by the number of cells of gross thickness, 29 (= 38/1.31), and was designated as KDR_1 (Eq. 6). In order to examine the influence of the transition zone, KDR_2 was also measured by counting the number of cells that the knot and transition zones encompassed (Eq. 7).

$$\mathrm{KDR}_1 = \frac{n_{knot}}{n} \tag{6}$$

$$\mathrm{KDR}_2 = \frac{n_{knot} + n_{transition}}{n} \tag{7}$$

where n_{knot} is the number of mesh grid cells encompassed by knot in an X-ray path; $n_{transition}$ is the number of cells encompassed by the transition zone in an X-ray path; n is the number of cells for 38 mm of thickness (29 cells).

Prediction of ratio of knot area to cross-sectional area

The KDR value provides one-dimensional knot information. In contrast, compressive strength and tensile strength are expected to be related to the area of knot in a cross section, which is two-dimensional information.

By using Eq. 8, the ratio of knot area to cross-sectional area (AR_x), two-dimensional information, was calculated.

$$\mathrm{AR}_x = \frac{\sum_{i=1}^{n} \mathrm{KDR}_i}{n} \tag{8}$$

where AR_x is the ratio of knot area to cross-sectional area predicted by X-ray analysis; KDR_i is the predicted knot depth ratio of the i-th pixel in a cross section; n is the number of pixels for a cross section. Because the resolution of 1.31 mm/dot was used, the value of 29 was applied.

In order to investigate the accuracy of AR prediction, the real area ratio was calculated (Eq. 9):

$$\mathrm{AR}_{real} = \frac{A_{knot} + A_{transition}}{A} \tag{9}$$

where AR_{real} is the ratio of knot area including transition zone to cross section determined by observing the cross section; A_{knot} is the number of mesh grid cells encompassed by knot in a cross section; $A_{transiton}$ is the number of mesh grid cells encompassed by transition zone in a cross section; A is the number of cells for the cross section.

Results and discussion

Measurement of knot density for an input variable of KDR prediction

Figure 7 shows the result of density prediction using X-ray radiation. Both specimen groups of 10 and 38 mm in thickness showed a significantly strong relationship between the predicted density and the air-dry density.

X-ray images for knot and transition zones were extracted from raw X-ray images of Japanese larch and red pine. Each density was obtained by converting each cell of the partial image for each zone. Table 2 shows the statistics of knot densities for two of the species tested. The densities of the knot and transition zones for two types of knots – tight knots and encased knots – were calculated using Beer's Law. The X-ray image for the transition zone of the encased knot could not be extracted because the width of the transition zone was too small. The average density was 0.95 g/cm^3 for Japanese larch and 0.93 g/cm^3 for red pine. Average densities were approximately double the density of clear wood.[12]

A *t*-test was carried out to investigate the similarity of transition zone density to knot density. It was hypothesized that there is no difference between knot density (μ_1) and transition zone density (μ_2): null hypothesis $H_0: \mu_1 = \mu_2$

A two-tailed test with a significance level of 0.10 was conducted. If a test statistic is larger than the *P*-value, H_0 is rejected. However, the two-tailed test showed that the densities of knot and transition zone were not different from each other in terms of a 10% significance level (H_0 accepted, Table 3). When the X-ray image was observed by the naked eye, the transition zone and knot were not identified. This was considered to be caused by the similarity in density. Because the density of the transition zone is similar to knot density, the average density was used for the input variable of KDR calculation.

Verification of KDR evaluation method

Comparison of KDR_x and KDR_1

To verify the proposed KDR method, KDR_x and KDR_1 were compared (Fig. 8). The KDR_x predicted by the proposed method commonly overestimated the KDR_1. It was speculated that the dense transition zone caused this overestimation. The density of the transition zone is similar to the knot density (see Tables 2 and 3). This overestimation was prominent for low values of KDR_1. A cell with a low

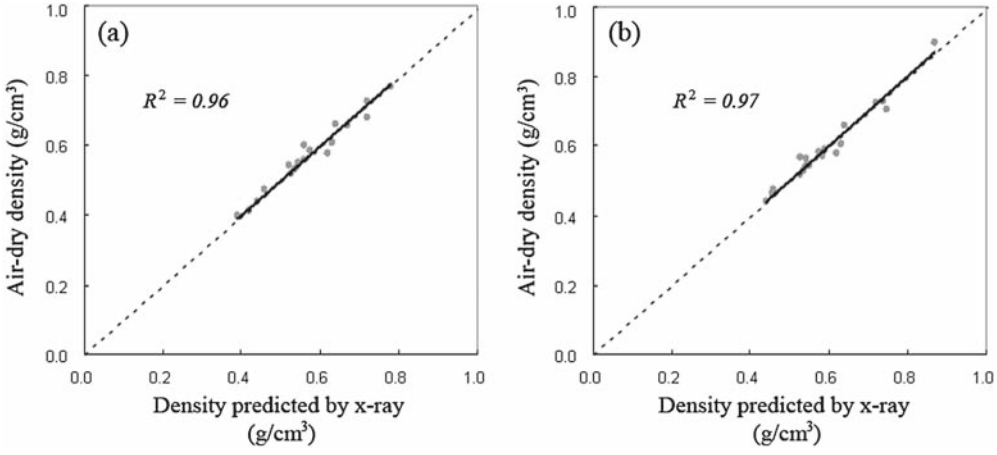

Fig. 7a, b. Relationship between the density prediction by X-ray radiation and air-dry density. **a** The 10-mm-thick specimens. **b** The 38-mm-thick specimens

Table 2. Knot density for two tree species

Species	Sample zone	Knot				Average knot density (g/cm^3)	Clear wood density (g/cm^3)
		Tight knot		Encased knot			
		Number of knots	Average density (g/cm^3)	Number of knots	Average density (g/cm^3)		
Japanese larch	Knot	32	0.96 (0.132)	22	0.96 (0.102)	0.95	0.48
	Transition		0.93 (0.182)				
Red pine	Knot	23	0.93 (0.097)	19	0.93 (0.089)	0.93	0.44
	Transition		0.92 (0.173)				

Values given in parentheses are standard deviations

Table 3. Result of *t*-test for difference between knot density and transition zone density

Species	Sample zone	Tight knot	*t*-test		
		Average density (g/cm^3)	Test statistic	*P*-value[a]	Result
Japanese larch	Knot	0.96 (0.132)	1.35	1.65	H_0 accepted
	Transition	0.93 (0.182)			
Red pine	Knot	0.93 (0.097)	0.95	1.65	H_0 accepted
	Transition	0.92 (0.173)			

Values given in parentheses are standard deviations
[a] Probability that absolute value is larger than *P*-value is 0.10 in *t*-distribution

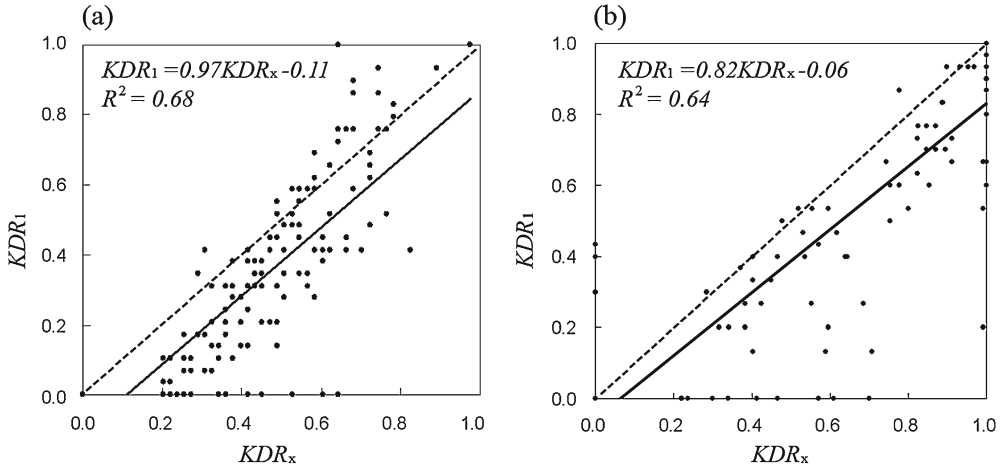

Fig. 8a, b. Relationship between the predicted knot depth ratio (KDR_x) and KDR_1, which is the ratio of knot to lumber thickness. **a** Japanese larch, **b** red pine

KDR_1, for example, section B-B' in Fig. 9a, has a relatively large transition zone. Section B-B' has a smaller transition zone than section A-A'; however, the amount of knots in section B-B' is much smaller than that in section A-A'. In low KDR_1 cells, the ratio of the transition zone ($t_{transition}$ / t_{knot}, Fig. 9a) is relatively large.

In the case of Japanese larch, the cells with KDR_1 close to 1.0 were not overestimated; rather, they were underestimated (Fig. 8a). To find the cause of this underestimation, the diameter of knots in appearance of lumber was investigated. The knots with diameters smaller than 20 mm were ignored in knot diameter measurement. In the case of Japanese larch, 99.4% of knots were smaller than the lumber thickness of 38 mm. This indicates that the knots with KDR_1 close to 1.0 have a special geometric shape in that the knot axis and the wide face of the lumber are almost at a right angle (Fig. 9c). In the case of this special knot geometry, the cells had no transition zones in the X-ray path; therefore, no overestimation was expected to occur in cells with KDR_1 close to 1.0. In addition, most knots contained cracks (Fig. 10). Because of the special knot geometry found in the knots with cells with KDR_1 close to 1.0, the reduction in X-ray attenuation by the cracks caused the cells with larger KDR_1 values to be severely underestimated.

In the case of red pine, however, it has larger knots than Japanese larch. In the knot diameter investigation, only 43.4% of red pine knots were smaller than the lumber thickness of 38 mm. Even though the knot axis and wide face were not at a right angle, a KDR_1 value of 1.0 can exist (section C-C' in Fig. 9b). From these statistics of knot diameter, it can be inferred that the knots with larger KDR_1

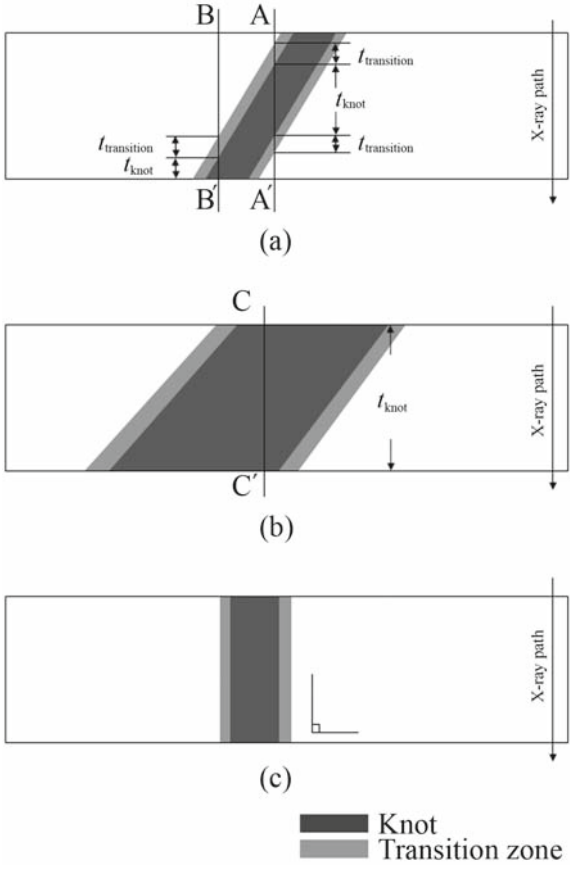

Fig. 9a–c. Cross-sectional views of different shapes of knots and the effect of transition zone and knot size on KDR evaluation. **a** Small-diameter knot, **b** large-diameter knot, **c** possible geometry of knot in the case where small-diameter knot has KDR close to 1.0

values do not have a special geometry but have various geometries. Even though some cells may be underestimated due to cracks found in knots, no overall tendency for underestimation was found (Fig. 8b).

Comparison of KDR_x and KDR_2

Because it was speculated that the transition zone would cause overestimation of KDR_1, the KDR_x value was compared from the ratio of the knot and transition zone to the lumber thickness, KDR_2. Figure 11 shows strong relationships between KDR_x and KDR_2 for Japanese larch and red pine, with R^2 values of 0.87 and 0.83, respectively. The slope of the regression curve was close to 1.0 (dashed line). These results demonstrated that the proposed knot depth ratio prediction method is more suitable for evaluating KDR_2 including the transition zone. Unfortunately, it cannot predict the ratio of knot in lumber thickness, and it involves transition zone as well as knot.

Even though redefining the KDR increases its accuracy, the misleading effect of cracks in knots, as in the Japanese larch specimens, still remains (Fig. 11a) and these errors are expected to occur in the analysis of other species containing small-diameter knots.

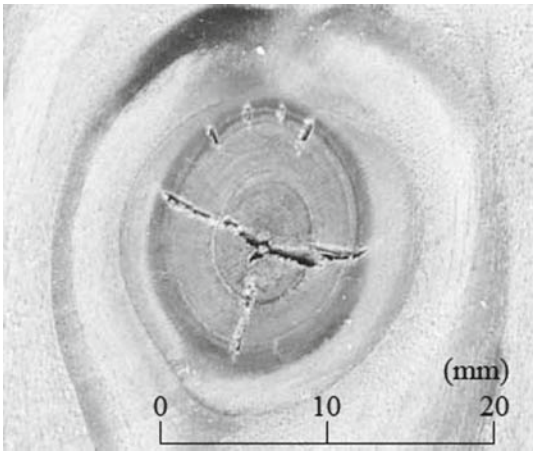

Fig. 10. Example of knot containing cracks (Japanese larch)

Prediction of ratio of knot area to cross-sectional area

Generally, it was assumed that knots reduce the effective cross-sectional area with regard to strength. Therefore, the relative ratio of knot was targeted for prediction. Because the KDR method gives the KDR values for knot zone including transition zone, the knot area ratio predicted by X-ray also contains the transition zone area.

The ratio of knot and transition zone area to the cross-sectional area was calculated from X-ray image analysis. The predicted area ratio (AR_x) was compared with the real area ratio (AR_{real}) defined as the ratio of knot and transition zone area to the gross cross-sectional area.

Figure 12 shows the relationship between the predicted area ratio and the actual area ratio, which is more successful than the KDR prediction. It was speculated that the annual rings cause the increase of coefficient of determinant. There are various geometries of annual rings due to the sawing method, including edge grain and flat grain lumber (Fig. 13). If an X-rays pass through the tangential direction in edge grain lumber (Fig. 13a), the latewood and earlywood can be identified in the X-ray image because latewood density is higher than that of earlywood. If latewood and knot exist together in the path of X-rays, the X-ray image analysis would overestimate the KDR value; conversely, earlywood causes it to be underestimated. Fortunately, latewood and earlywood coexist in a repeated fashion. If a cross section has cells that have been overestimated due to latewood, it may also have the underestimated cells. It was considered that the extent of underestimation and overestimation was nearly identical in a cross section. The effect of the repeated underestimations and overestimations caused by latewood and earlywood is thought to be minimized by their cancellation of each other.

Ultimately, it can be concluded that X-rays can be used to quantify knot area in a cross section, considering the R^2 values of 0.89 for Japanese larch and 0.93 for red pine, even though the different density of latewood and earlywood affects the KDR calculation and reduces the accuracy. Because the KDR_x value involves transition zone, the area ratio predicted by X-ray image analysis also includes the transition zone area as well as knot area.

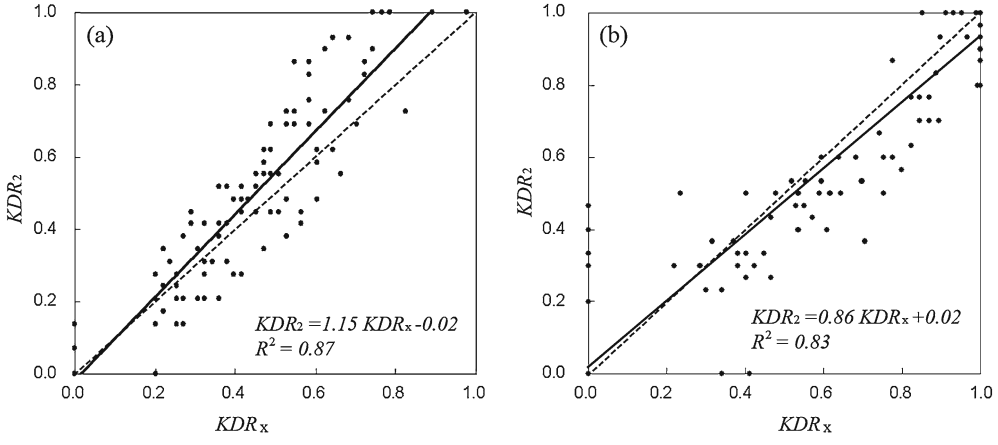

Fig. 11a, b. Relationship between KDR_x and KDR_2, which is the ratio of knot and transition zone to lumber thickness. **a** Japanese larch, **b** red pine

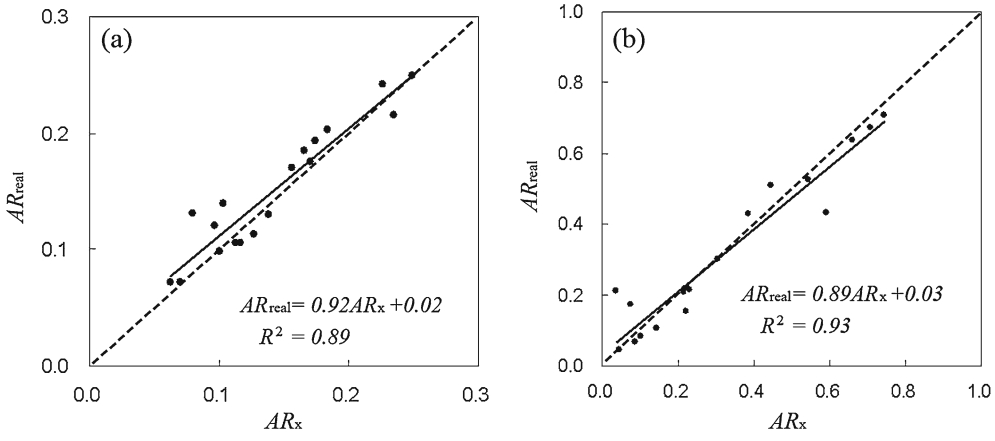

Fig. 12a, b. Relationship between the real area ratio (AR_{real}) and the predicted area ratio (AR_x). **a** Japanese larch, **b** red pine

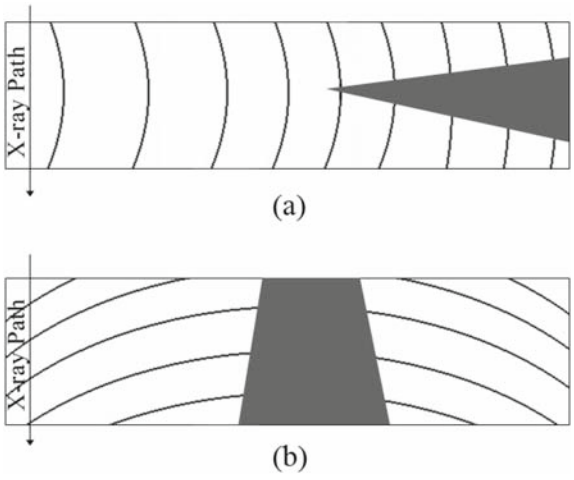

Fig. 13a, b. Geometry of the annual ring and the knot according to sawing type. a Edge-grain lumber, b flat-grain lumber

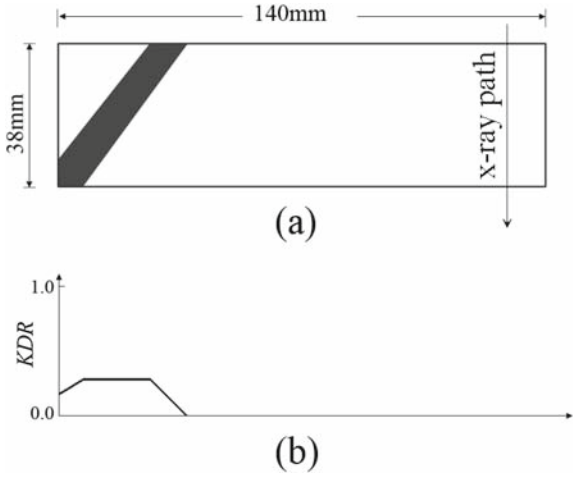

Fig. 14a, b. Geometric meaning of the knot depth ratio evaluation method. **a** Cross-sectional view of an example of a knot, **b** KDR information

Even though this method cannot provide the exact location of knots in 38 mm of thickness (Fig. 14), the KDR method allows the evaluation of the knot area in a certain cross section and to identify the exact location of knot in a 140-mm width. In additional, this method requires only a single X-ray radiation. This differs from computed tomography, which uses a number of X-ray radiations.

In order to use the KDR evaluation method for grading or predicting strength, further studies on the relationship between strength and KDR are required, because the KDR values involve the transition zone as well as knots.

Conclusions

In this study, the knot depth ratio (KDR) evaluation method was proposed. This method was developed to quantify the geometric amount of knots in a cross section, using a single-pass X-ray radiation. To verify the proposed method, the KDR values for 38-mm-thick lumber were evaluated. After comparing the predicted KDR values with the real KDR values measured by observing the cross section, the conclusions are:

1. X-rays cannot distinguish between knot and transition zone because the density of the transition zone is similar to that of the knots.
2. The KDR method can quantify the ratio of knot involving transition zone to lumber thickness. The KDR values for Japanese larch and red pine specimens were predicted by the proposed method with R^2 correlations of 0.87 and 0.83, respectively. However, underestimation of KDR caused by cracks in the knots still remains and further studies for various species with small-diameter knots are required.
3. In the KDR evaluation, the difference of density between latewood and earlywood in the same path of the X-rays causes estimation discrepancies. However, when the ratio of knot area to cross-sectional area was calculated using KDR information, the discrepancies were effectively canceled out because latewood and earlywood are repeated. Evaluation of the area ratio using KDR information increased the correlation between the predicted KDR and the real KDR with R^2 values of 0.89 and 0.93 for Japanese larch and red pine, respectively.

Acknowledgments This study was carried out with the support of Forest Science and Technology Projects (Project No. S120708L1001104) provided by the Korea Forest Service.

References

1. Riberholt H, Madsen PH (1979) Strength of timber structures, measured variation of the cross sectional strength of structural lumber. Report R 114, Structural Research Laboratory, Technical University of Denmark
2. Schniewind AP, Lyon DE (1971) Tensile strength of redwood dimension lumber II. Prediction of strength values. Forest Prod J 21:45–55
3. Johansson CJ, Brundin J, Gruber R (1992) Stress grading of Swedish and German timber. A comparison of machine stress grading and three visual grading systems. Swedish National Testing and Research Institute, SP Report 1998:38
4. Machado JS, Sardinha RA, Crus HP (2007) Feasibility of automatic detection of knots in maritime pine timber by acousto-ultrasonic scanning. Wood Sci Technol 38:277–284
5. Baradit E, Aedo R, Correa J (2006) Knots detection in wood using microwaves. Wood Sci Technol 40:118–123
6. Gerhards CC (1982) Effect of knots on stress waves in lumber. Research Paper FPL-RP-384. USDA Forest Products Laboratory, Madison, WI, USA
7. Hu C, Tanaka C, Ohtani T (2004) Location and identifying sound knots and dead knots on sugi by the rule-based color vision system. J Wood Sci 50:115–122
8. Lam F, Barrett D, Nakajima S (2005) Influence of knot area ratio on the bending strength of Canadian Douglas fir timber used in Japanese post and beam housing. J Wood Sci 51:18–25
9. Madsen B (1992) Structural behaviour of timber. Timber Engineering, pp 52–79
10. Institute of Isotopes of the Hungarian Academy of Sciences (1986) Industrial application of radioisotopes. Elsevier, Amsterdam, pp 232–239
11. Kim KM, Lee SJ, Lee JJ (2006) Development of portable X-ray CT system I – evaluation of wood density using X-ray radiography. J Korean Wood Sci Technol 34:15–22
12. Sahlberg U (1995) Influence of knot fibers on TMP properties. TAPPI J 78:162–168
13. Oh JK, Kim KM, Shim K, Park JH, Kim WS, Yeo H, Lee JJ (2007) Prediction of bending performance for Japanese larch lumber: X-ray scanning. Proceedings of the Korean Society of Wood Science and Technology Annual Meeting, Yeosu, pp 71–72
14. Kim KM, Lee SJ, Lee JJ (2006) Development of portable X-ray CT system II – CT image reconstruction of wood using density distribution. J Korean Wood Sci Technol 34:23–31
15. Lee SJ, Kim KM, Lee JJ (2006) Application of the X-ray CT technique for NDE of wood in field. Key Eng Mater 321–323:1 172–1176
16. Rojas G, Condal A, Beauregard R, Verret D, Hernandex RE (2006) Identification of internal defect of sugar maple logs from CT images using supervised classification methods. Holz Roh Werkst 64:295–303
17. Korean Standards Association (2002) Softwood structural lumber, KS F 2162
18. Western Wood Products Association (2005) Western lumber grading rules 05. pp 143–148